*Materials Science Forum Vols. 235-238 (1997) pp. 5-14*
*online at http://www.scientific.net*


# Distinct Element Modelling of Mechanical Alloying in a Planetary Ball Mill

M.P Dallimore and P.G. McCormick
Research Centre for Advanced Mineral and Materials Processing
University of Western Australia
Nedlands, WA 6907 Australia

Keywords: mechanical alloying, planetary ball mill, distinct element modelling, mechanochemical reactions

The distinct element method (DEM) of modelling interactions in particulate systems has been used to analyse the motion of grinding media in a planetary ball mill. A two dimensional computer simulation has been developed which incorporates a modified Kelvin viscoelastic spring/damper system to model the impact process using experimentally derived collision parameters. The model enables quantitative analysis of the collision energies and their spatial distribution. The results of the model have been compared with experimental measurements of the effect milling parameters have on the kinetics of the CuO/Ni displacement reaction.

## Introduction

Many types of laboratory scale mechanical mills are used in the study of mechanical alloying (MA). These include shaker mills, attritors, tumbling mills and planetary mills. Planetary mills, in particular, have been extensively studied[1, 2, 3]. This can be attributed to the relatively ordered motion of the media and high processing rates attainable in these mills.

Planetary mill motion involves the rotation of a planetary arm about a central axis. Placed at the end of the arm is the milling chamber or vial which rotates about a second axis which is parallel to the mill axis. Commercially available laboratory scale mills typically fix the secondary rotation as a negative multiple of the primary rotation.

This paper describes the adaptation of distinct element method (DEM) modelling to the analysis of ball motion of planetary milling systems. A two dimensional model is presented which is capable of predicting the motion of the balls within the vial and the collision energy dissipated during milling. The model has been used to predict changes in ball motion and energy dissipation when varying numbers of balls are used in the milling. These predictions have then been compared to the kinetics of the CuO/Ni displacement reaction propagated via these conditions.

## Distinct Element Method Modelling

DEM modelling is a numerical method of analysing the behaviour of a system of distinct elements contained within a defined boundary over a series of small time steps. The independent nature of the elements allows them to be displaced and rotated in response to applied forces. These forces result from both interactions between the elements and external sources such as gravity. The aim of DEM modelling is to produce a displacement-time history for each element in the system.

The repetitive algorithm used in DEM modelling is initiated by considering all existing interactions between the elements and the elements and the boundary. Each interaction is assessed to determine the resulting contact forces. Each element is then considered individually, the interaction forces acting on that element are summed, and to this is added any externally derived forces. With the total force known, the acceleration of the element is found. This acceleration is then integrated over the time interval to determine the velocity and displacement of the element at the beginning of the next time step. The time step is then incremented and the elements moved to their new locations before the process is repeated.

DEM modelling is based upon the assumption that the system being modelled will remain stable for the duration of each time step. That is, the state of the system at the beginning of the next time step can be determined from the state of the system during the current time step. A suitably small time step must therefore be chosen.

The first application of DEM modelling was in the field of Geomechanics. Cundall and Strack developed the method for their work in simulating granular assemblies [4]. Their model used a system of distinct discs to represent various soil conditions. Interactions between the discs were modelled via Kelvin viscoelastic spring and dashpot couples .

DEM modelling is particularly suited to the analysis of the motion of grinding media in ball mills. This fact was first realised by Mishra et al [5] when DEM was used to predict the motion of

balls in horizontal tumbling mills. Their work also utilised the Kelvin model to simulate impacts and has since been extended to predict torque requirements in tumbling mills [6].

**The DEM Model of a Planetary Ball Mill**

A two dimensional model has been designed to predict the motion of the balls for any configuration of planetary mill. The implementation of the DEM of modelling in the program PMILL is outlined below.

As with all DEM models of ball mills, the balls within the vial are treated as distinct elements while the vial walls bound the system. Due to the translating/rotating motion of the vials inherent in planetary mills, a rotating reference frame is used to simplify the way that the vial is viewed. The reference frame rotates with the same angular velocity as the planetary radius and is situated at the centre of the vial. As a result, the translational motion of the vial is negated and the vial appears to rotate with an angular velocity equal to the vector difference of the vial and planetary arm angular velocities.

The motion of the balls is now described relative to the rotating reference frame. Consequently, the balls will be subjected to relative accelerations resulting from the motion of the reference frame [7]. These pseudo-gravitational accelerations scale directly with mill speed and this is the basis of predictions made by kinematic models of planetary systems that ball trajectories are independent of mill speed [1].

The basic repetitive algorithm of PMILL requires that the position and velocity of the balls be defined at the start of each time step. This is initially achieved by placing the balls in a hexagonal close packed matrix, the size of which is determined by the number of balls included in the simulation. From this point a list of all ball-ball and ball-wall contacts is produced. This is simply done by comparing the position vectors of each ball with every other ball and the vial radius. The contact list is compared with the list generated in the previous time step to determine which contacts are new, which are continuing from previous time steps, and which have ceased. Initial impact conditions for the new contacts are recorded while information on contacts terminated during the previous time step is written to file.

A temporary local normal-tangential coordinate system is then defined for each contact. The impact force is then calculated in the two component directions. The method used to determine the magnitude of the impact force components is described in the next section. Once determined these forces are then converted back to the global rotating reference frame. This allows all impact forces acting on the individual balls to be easily summed. To this value is added the pseudo-gravitational forces. This yields the total force and net moment acting on each ball. It is then a simple matter of applying Newton's second law to determine the linear and angular acceleration of the balls.

With the use of an appropriately sized time interval ($\sim 10^{-6}$s), it is assumed that the acceleration of the balls will remain constant for the duration of the time step. This is the defining step of all DEM models. Such an assumption simplifies the integration procedure required to predict the velocities and position of each ball at the beginning of the next time step. The time step can then be incremented and the algorithm repeated.

**Modelling the Impact Process**

Two types of impacts are defined in the program PMILL. A ball-ball impact is recorded between two balls when the distance between their centres is less than the sum of their radii. For these impacts the normal direction is defined by a vector from the centre of the first ball to the centre of the second. A ball-wall impact is recorded when the magnitude of the position vector of a ball is greater than the difference between the radius of the vial and the ball. In this case the normal direction is defined by the position vector of the ball involved. For both types of impact the tangential direction is defined by an anticlockwise rotation of the normal vector and thus lies parallel to the contact surface. Impact forces are generated at the contact interface that act to separate the elements. The validity of the model will be influenced by the way in which these forces are evaluated.

As stated above, previously developed DEM models of ball milling devices have utilised Kelvin viscoelastic couples to calculate the restoring forces occurring in the normal direction. The couple consists of parallel spring and dashpot components. The spring, of stiffness $K_n$, supplies a repulsive force proportional to the amount of overlap of the elements. It thus stores energy as the two elements approach before returning it as the elements separate. The energy absorbed by the dashpot is dissipated during the collision and is calculated as the product of the damping coefficient $C_n$ and the value of the relative velocity of the two elements.

To more accurately reflect the geometry of the spherical elements, PMILL uses a modified version of the Kelvin model when evaluating normal forces ($F_n$). The modified model may be visualised as a series of concentric parallel pairings of springs and dashpots, the number of which are included in the calculation being dependent upon the amount of overlap between the colliding elements. Thus the elastic component of the normal force is proportional to the volume of the overlap ($\delta$vol) while the damping component is proportional to both the velocity of approach and the instantaneous area of the impact ($\delta$a). To further enhance the relevance of the model to mechanochemical processes, the damping portion of the impact force is only calculated during the approach of the two elements and is thus used to represent the loss of energy associated with plastic deformation of the powder trapped in the collision. The equation for the normal force becomes

$$F_n = \hat{K}_n * \delta vol + \hat{C}_n * v_n * \delta a \qquad \text{as elements approach}$$

$$F_n = \hat{K}_n * \delta vol \qquad \text{as elements separate} \qquad \text{Eqn 1}$$

The spring and dashpot coefficients are denoted $\hat{K}_n$ and $\hat{C}_n$ and have units of $Nm^{-3}$ and $Nsm^{-3}$. As the model is only an approximation of the impact process, contact overlap and volume are calculated as simple geometric functions of the degree of overlap. This simplifies the computational procedure.

In modelling the tangential impact forces, a dry friction slider has been placed in series with a Kelvin viscoelastic couple to allow for sliding of the elements at the collision interface. The viscoelastic couple is described by the spring constant $K_t$ ($Nm^{-1}$) and the damping coefficient $C_t$ ($Nsm^{-1}$). No relative motion will occur between the contact surfaces until the friction force, which is calculated by the product of $F_n$ and a friction coefficient ($\mu$) is surpassed by the calculated viscoelastic force. Once sliding occurs, the tangential force is set equal to the friction force.

**Characterisation of Impact Coefficients.**

The success of the impact model described above depends upon realistic coefficients being specified for the viscoelastic and friction components. This has been achieved by measuring the force response of a single impact and evaluating the level of friction occurring between the balls and the vial wall during milling.

Normal impact forces were isolated with the aid of a simple free fall experiment. This involved dropping a ball from a known height onto the vial surface which was rigidly mounted on top of a force transducer. The signals generated by the force transducer were then used to evaluate the coefficient of restitution (e) and the force distribution over the duration of the impact. A simplified version of the PMILL code was then used to iteratively fit the normal coefficients $\hat{K}_n$ and $\hat{C}_n$ to the measured values of e and impact duration. Note that all experiments were conducted with the balls and vial coated with powder to more realistically reflect actual milling collisions. A value of e=0.5 was measured and was found to be sufficiently stable over a range of impact velocities for a given powder thickness. A more detailed description of this measurement and the results obtained have been published previously [8]. The values of $\hat{K}_n$ and $\hat{C}_n$ have been set at $3250*10^{10}$ $Nm^{-3}$ and $700*10^{6}$ $Nsm^{-3}$ for all simulations where e=0.5.

Variations in e will occur for varying thickness of powder trapped between the balls during impact [9]. To account for the possibility of a greater powder thickness occurring on the walls of the vial during milling, a basic sensitivity analysis is included latter in this paper. For these simulations the value of e was set to 0.3 by adjusting $\hat{C}_n$ to $1800*10^{6}$ $Nsm^{-3}$.

The value of $\mu$ to be used in the simulation was measured with the use of a pin-on-disk machine. To establish a coherent powder coating, the vial and balls were premilled before $\mu$ was measured. The vial, when mounted in the pin-on-disk machine, rotates about its central axis allowing a single ball to be pressed against it's surface with a known normal force. By measuring the resistance to sliding, $\mu$ is easily calculated. Using angular speeds and normal forces similar to those predicted to occur inside the planetary mill, the value of $\mu$ was measured at 0.65 [8].

As it is extremely difficult to design an experiment that isolates the viscoelastic portion of a purely tangential collision the values of $K_t$ and $C_t$ have been taken from the normal impact measurements. Values of $K_t$ and $C_t$ have been set at $17.3*10^{6}$ $Nm^{-1}$ and 460 $Nsm^{-1}$. This is a similar approach to that used by both Cundall and Strack [4] and Mishra et al [5].

**Experimental Procedure and Results**

The aim of this series of experiments has been to determine the optimum number of balls to include in the charge for the most efficient propagation of a typical mechanochemical reaction.

The reaction considered is the displacement reaction Ni + CuO ⇒ Cu + NiO. The progress of this reaction is easily monitored by measuring the saturation magnetisation ($M_S$) of the as-milled powder. As nickel is the only ferromagnetic component of the reaction, the value of $M_S$ is directly proportional to the remaining fraction of nickel ($f_{Ni}$). The reaction may also be milled in air without distortion of its pathway.

Milling was conducted in a Fritsch Pulvisette 5 mill. The planetary arm measures 0.122m and the vials rotate with an absolute angular velocity of -1.25 times that of the planetary arm. Hardened steel vials, with an internal diameter of 64mm, have been manufactured to contain the milling charge which is comprised of 12.7mm chrome steel balls and the powder to be processed. The depth of the vials has been set to 15mm to effectively restrict the motion of the balls to the horizontal plane. This improves the relevance of the two dimensional model outlined above.

Adopting the convention previously described in the literature [10], the number of balls is characterised by the filling fraction,

$$n_v = \frac{N_b}{N_{b,max}} \qquad \text{Eqn 2}$$

where $N_b$ is the number of balls included in the vial and $N_{b,max}$ is the maximum number of balls, of the specified size, that could be included in the vial. Here $N_{b,max}$ =19. The number of balls used in the experiments was varied between three and sixteen giving a variation in $n_v$ from 0.16 to 0.84. The various configurations of the mill were used to process a 3g stoichiometric mixture of Ni and CuO. This resulted in a variable charge ratio (mass of balls to mass of powder).

Fig 1 plots the level of $f_{Ni}$ after three hours milling at 300 revolutions per minute as a function of the number of balls included in the vial. The plot shows that increasing the number of balls initially increased the reaction rate. A maximum rate was achieved at $n_v$=0.42. Increasing $n_v$ to higher values clearly resulted in a decrease in milling efficiency.

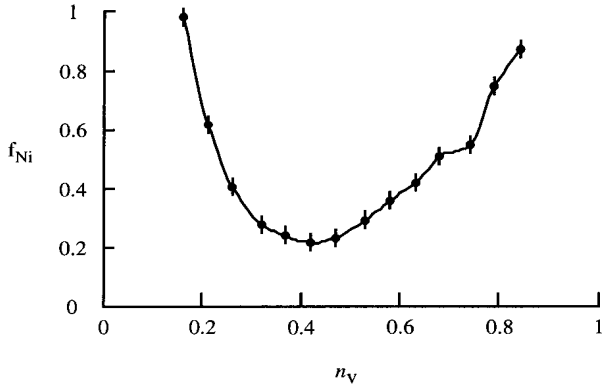


Fig 1: Fraction of nickel remaining in the charge after three hours of milling at 300rpm as a function of $n_v$.

**Simulation Data Analysis**

Numerical trials have been conducted to mirror the displacement reaction experiments. Each trial was conducted for a total of 505 revolutions in the rotating reference frame. The first five revolutions allowed the motion of the balls to become established. Collision data was then collected for the remaining 500 revolutions. The predicted changes in ball motion and relative energy dissipation for varying numbers of balls is now discussed.

***Ball Motion***. Increasing the number of balls present in the vial reduced the amount of slip experienced by the balls as they moved from the toe of the charge to the departure point at the shoulder of the charge. The level of slip is defined by a slip factor $f_s$ which is calculated as

$$f_s = 1 - \frac{D_{actual}}{D_{no\_slip}} \qquad \text{Eqn 3}$$

where $D_{actual}$ is the number of departures from the shoulder of the charge predicted by the simulation and $D_{no\_slip}$ is the number of departures that would occur if no relative motion between the balls and the vial wall existed. Using this definition, $f_S$=0 when no slip occurs and $f_S$=1 when there is no tumbling in the mill. Fig 2 shows the variation in slip as a function $n_v$.

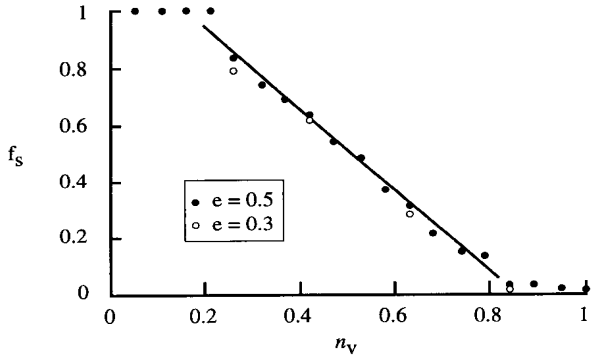


Fig 2. Slip factor, $f_s$ , as a function of $n_v$. The sensitivity of the model to changes in the value of the modelled coefficient of restitution is reflected in the two sets of data.

When three balls only are simulated ($n_v$=0.16), the model predicted that balls will roll on the bottom of the vial without tumbling. The balls simply remain at the point of lowest potential energy. The four ball simulation ($n_v$=0.21) also predicts rolling of the balls. During this simulation the balls align with three of the balls against the bottom of the vial while the fourth rolls in a secondary layer on top of the others. The rolling predicted in these simulations is stable and continuous. This resulted in only a few long duration, and thus high energy, impacts being recorded by PMILL. This stability of the rolling phases will be reduced in reality due to naturally occurring variations in the milling process such as differences in powder thickness. This is likely to result in periods of intermittent tumbling and rolling for these low filling fractions.

For $n_v$ greater than 0.21, continuous tumbling of the balls resulted. The tumbling motion can further be divided into cataracting and cascading motion. Cataracting implies that the balls departing the shoulder of the charge, will tumble unimpeded to the toe of the charge where they impact either the vial wall directly or a ball resting against the vial wall. Cascading describes the motion of a tumbling ball that reaches the foot of the charge in a series of lesser impacts. Both forms of tumbling were present in all simulations where tumbling is predicted.

The decrease in slip that resulted from the addition of more balls to the simulation does increase the departure velocity of balls leaving the shoulder of the charge. This gives a wider arc to the trajectory of the tumbling ball pushing it further across the vial and promoting cataracting in the mill. However the increased bulk of the charge reduced the chance that the ball will be unimpeded in its flight to the impact zone. Thus there was a trend away from cataracting to cascading as more balls were introduced into the simulation.

The changes occurring in mill motion can be illustrated by considering the spatial distribution of impact frequency. Fig 3 shows this distribution for a range of vial filling fractions ($n_v$=0.26, 0.42, 0.63 and 0.84). These plots have been constructed by dividing the vial space into a 41x41 matrix with each impact being assigned to an element according to the impact point of the collision.

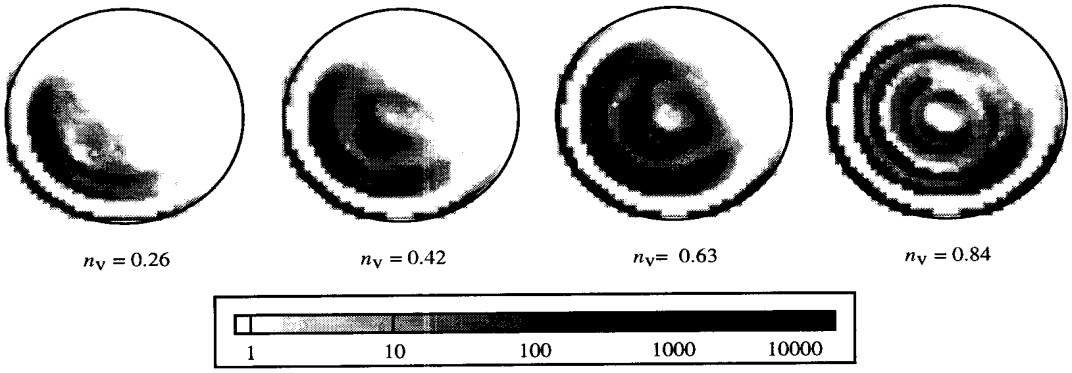


Fig 3. Predicted impact frequency spatial distributions for a range of vial filling fractions. The impacts occurred during 500 revolutions in the rotating reference frame

It can be seen that the shoulder of the charge moved up the vial wall as $f_s$ decreased. The toe of the charge also moved higher up the wall in part due to the increase in departure velocity associated with the decrease in $f_s$ but more predominantly due to the increase in size of the charge. A trend towards an ordered tumbling motion can also be seen with the clarification of the distinct impact bands occurring in the charge as the number of ball is increased.

***Energy Dissipation.*** The predicted energy dissipated in the dashpots and friction slider for each collision during the simulation was recorded for analysis. This data is presented in several formats.

*Combined Energy Dissipation.* Fig 4 plots the sum of all energy dissipated in the normal and tangential directions. It can be seen that once tumbling occurred, the predicted normal impact energy increased with the number of balls included in the mill until a maximum was reached at $n_v$=0.63. The predicted levels of tangential energy peaked $n_v$=0.37 before tapering off at higher $n_v$. When the two components were summed, a maximum total energy was predicted for $n_v$=0.58.

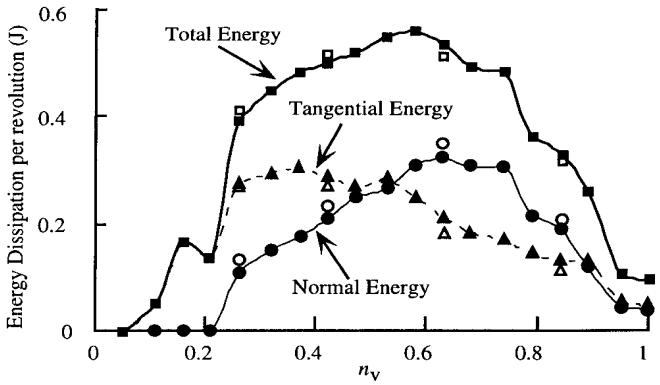


Fig 4. Predicted energy dissipation as a function of $n_v$. The sensitivity of the model to changes in the coefficient of restitution, e, is indicated by the two sets of data. The closed symbols represent predicted values for e = 0.5. The open symbols represent predicted values for e = 0.3.

*Energy Dissipation Spatial Distributions.* To understand the mechanisms of normal and tangential energy dissipation predicted by the simulations, energy dissipation spatial distributions can be used. Again the vial space has been divided into a 41x41 square matrix, this time the energy dissipated for each collision being assigned to an element according to the collision impact point These plots show the sum of all energy dissipated in the elements and highlight the regions within the vial where the normal and tangential energy is most heavily dissipated (Fig 5).

The spatial distributions for the simulation trials where tumbling is the prevalent motion show that the areas of highest normal impact energy dissipation occurred at the toe of the charge. This is as expected as these regions represent the impact zones of balls with the highest kinetic energy which have been thrown from the shoulder of the charge. Two clear impact zones are present for $n_v$=0.42 and $n_v$=0.63. The first lies on the vial wall and represents ball-wall collisions. These collisions included direct strikes from tumbling balls and secondary collisions from balls resting against the vial wall which have been impacted from above by cascading balls. The second impact zone occurs at the point of contact between cascading balls and balls resting against the vial . Note that when $n_v$=0.84, the interior impact zone has fragmented indicating a trend towards cascading. The tangential energy spatial distribution plot for the three lower filling fractions indicates that the majority of tangential energy was dissipated during the grinding action of the balls as they moved from the toe to the shoulder of the charge. This energy was dissipated through both ball-wall and ball-ball contact. The decrease in tangential energy at higher $n_v$ was due to the decrease in relative motion between the balls and the balls and vial wall. It therefore reflects the decrease in $f_s$ with $n_v$.

*Impact Frequency Distributions.* To gain further insight into the method of energy transfer, impact frequency distributions are considered. Fig 6 plots the impact collision frequency per rotation as a function of both the normal and tangential energy dissipated in the collision for the four simulations considered previously. Intervals of 1mJ have been used. This graph makes it possible to determine if energy was being dissipated by a large number of low energy impacts or a smaller number of high energy impacts.

The impact frequency histogram for normal dissipated energy shows the trend towards cascading as the number of balls added to the vial was increased. The highest normal energy impacts occur

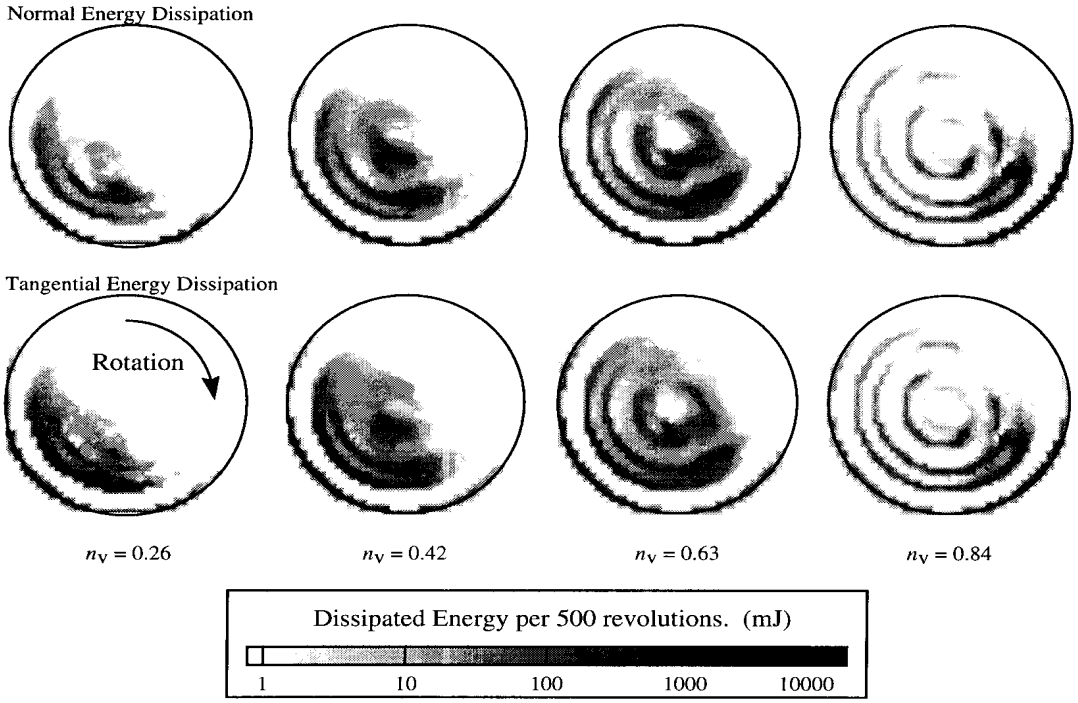


Fig 5: Predicted normal and tangential impact energy spatial distributions. The energy was dissipated during 500 revolutions in the rotating reference frame.

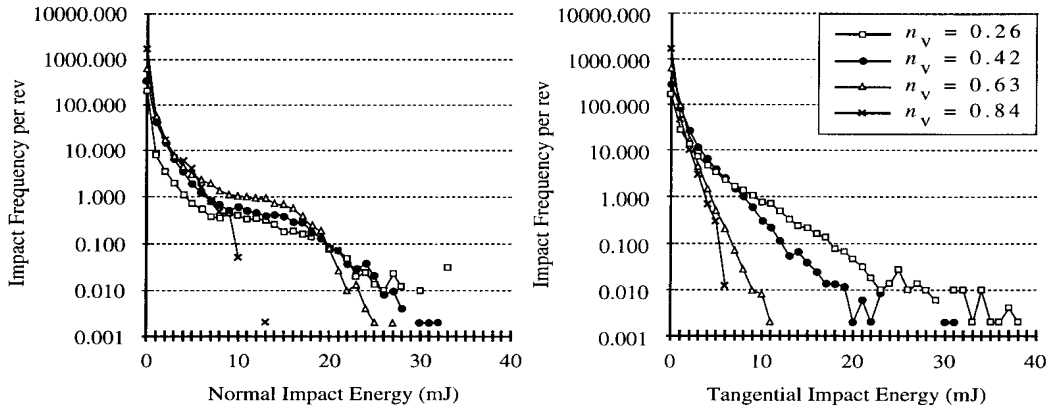


Fig 6. Impact frequeny per rotation as a function of both normal and tangential energy dissipated per impact.

for the simulation of the lowest filling fraction in which tumbling occurred. These impacts can be attributed to direct strikes in the impact zone by a tumbling ball. As the number of balls increased, the balls dissipated energy in a series of small impacts as they cascade down the charge face. This resulted in a trend away from smaller numbers of high energy impacts towards larger numbers of low energy impacts. The corresponding tangential impact energy histograms reveals the shift towards low energy tangential impacts at low levels of slip. This is accompanied by an increase in the total number of impacts which is due to the increase in $n_v$ required to reduce slip in the mill.

**Sensitivity Analysis**

The sensitivity of the simulation results to the level of damping has been evaluated. This analysis aims to highlight variations in the model predictions resulting from possible errors in impact characterisation experimentation. The value of e was altered to 0.3 for the simulations of four values of $n_v$, 0.26, 0.42, 0.63 and 0.84. This represents a significant variation from the measured value of e and can be regarded as an upper bound to the errors that may be expected.

Increasing the level of damping reduced the amount of rebound for every impact in the simulation due to the fact that more kinetic energy is removed from the ball. Consequently, balls reaching the toe of the charge begin moving back to the shoulder of the charge sooner. This had the effect of slightly reducing the predicted level of slip. The predicted slip values for the four high damping simulations have been included in Fig 2 where they are represented by open circles.

The change in ball motion predicted for higher levels of damping will clearly influence the dissipation of energy in the mill. Fig 4 shows variations in the combined energy dissipation resulting from the change to the assumed value of e. These points are distinguished by the use of open symbols. Increasing the damping, by decreasing the level of slip, increased the departure velocity of the balls resulting in higher levels of normal energy dissipation. The decrease in slip also reduced the relative motion of the balls as they move from the toe to the shoulder of the charge thus reducing the level of tangential energy dissipation. The net result is a slight shift in the total energy dissipation curve to the left.

The variations in the simulation results outlined above do not alter the underlying trends of the model's predictions. This demonstrates the robust nature of the model and confirms its suitability as a tool for investigating the propagation of MA processes. The sensitivity analysis presented here is by no means comprehensive. A more detailed study is currently being conducted.

**Discussion**

Kinematic models of planetary ball mills are typically constructed with the simplifying assumptions that no slipping of the balls moving up the vial wall to the departure point occurs and that no interference between tumbling balls is present. *In situ* and experimental observations have shown that these assumptions are invalid. Consequently, attempts have been made to incorporate empirically derived slip factors [11] and hindrance corrections [10] into the models to allow them to more accurately reflect the observed behaviour.

The benefit of DEM modelling lies in it's ability to analyse the motion of milling media without preconceived restrictions being applied to the motion of the balls. Instead, the assumption is made that all interactions between balls and the balls and vial wall can be modelled with the aid of experimentally evaluated viscoelastic couples and friction sliders. Thus variations in ball motion and the extent and type of energy dissipation can be qualified for different milling conditions.

Analysis of the simulation results has shown that PMILL predicted variations in ball motion at different values of $n_v$. The motion ranged from rolling at low values of $n_v$ to tumbling for medium to high values of $n_v$. A bias towards cascading at high $n_v$ was noted. The variation in mill motion that occurred can most easily be described by considering the level of slip in the mill. The value of $f_s$ was found to be a linear function of $n_v$. This can be explained by realising that without any form of lifters present in the vial, a ball will only move to the departure point if it is pushed there by other balls. The inclusion of more balls in the mill thus increases the speed at which a ball progresses from the toe to the shoulder of the charge. The decrease in slip had two effects upon the motion of balls. The first was to increase the departure velocity of the ball. For high $n_v$ the kinetic energy possessed by a tumbling ball approached the values assumed in kinematic models. The second effect on ball motion was to alter the flight path of the tumbling ball. Higher departure velocities threw the ball further across the vial, reducing the chance of interference between balls. However in the system studied, the larger values of $n_v$ required to reduce slip increased the bulk of the charge resulting in an increase in hindrance as more balls were added.

By definition, the slipping occurring in the vial effects the frequency of tumbling events. For the values of $n_v$ where tumbling was present, $f_s$ scaled directly to the number of balls until a value

of one was reached. This offers a possible explanation for the apparent validity of the assumption, made in kinematic models [1, 2], that the departure frequency scales to the number of balls .

The presence of slip also effected the way in which energy was dissipated in the model. The relative motion between the balls and the balls and the vial wall at low values of $n_v$, resulted in the largest portion of energy being dissipated by grinding of the balls as they move towards the departure point. This is reflected in the dominance of the tangential component of the dissipated energy up to $n_v$=0.5 shown in Fig 4 and the location of the energy dissipation shown in the spatial distributions for $n_v$ equal to 0.26 and 0.42 (Fig 5). Increasing $n_v$ resulted in the energy dissipated by impacts associated with tumbling events becoming the dominant mode of energy transfer. This is again shown in Fig 4 and Fig 5. At values of $n_v$ approaching one, the vial became over filled and prevented efficient head-on impacts from occurring. This resulted in the normal component of dissipated energy decreasing which is accompanied by a decrease in the total dissipated energy.

The predicted maxima in total energy dissipation with increasing $n_v$ discussed above is in good qualitative agreement with measurements of the power consumption of a Fritsch planetary mill reported by Iasonna and Magini [10]. They reported an increasing then decreasing level of power consumption for an increasing value of $n_v$. The work presented here thus confirms the link between the microscopic energy dissipation occurring during individual impacts and the macroscopic levels of mill power consumption.

The model will benefit MA research if it can provide information about how different milling configurations, and thus different impact conditions, affect a particular MA process. Comparison of the experimental and simulation results presented above provides an insight into the propagation of a typical displacement reaction by mechanical means. A comparison of Fig 1 and Fig 4 shows that the total level of energy dissipation and reaction rate exhibit the same qualitative dependence on $n_v$. When energy is dissipated purely by tangentially impacts, as occurs when rolling of the balls dominates the motion, low reaction rates were seen. A possible explanation may be that tumbling, which produces the high normal energy impacts, may be required to free powder encrusted on the vial wall, thus ensuring adequate mixing in the charge. The authors have previously suggested that the impact energy distribution is of little importance compared to the total level of dissipated energy [8]. These results further support this hypothesis.

## Summary and Conclusion

The motion of balls in a planetary mill has been modelled with the aid of the distinct element method. The impacts predicted by the model have been evaluated in terms of normal and tangential coordinates. A modified version of a Kelvin viscoelastic couple has been used to quantify the normal force while a serial combination of a conventional Kelvin couple and a dry friction slider are used to represent the tangential impact forces. Attempts were made to ensure the specified spring, damping and friction coefficients reflected actual milling conditions.

The developed model has been used to evaluate the way in which the motion of the balls and the energy dissipated varies in a typical laboratory scale mill for different filling fractions. These variations were explained by considering the predicted level of slip occurring between the vial and the balls moving to the impact point. The levels of predicted energy dissipation were in good qualitative agreement with measurements of mill power consumption reported in the literature.

The computational simulations were correlated with experimental measurements of the propagation of the CuO/Ni displacement reaction in a planetary mill. Comparison of the results lead to the conclusion that both tangential and normal components of energy dissipation are essential to the propagation of mechanochemical reactions in the planetary mill. The distribution of impact energies for varying filling fractions did not significantly influence the reaction rate.

## References


1. N. Burgio, A. Lasonna, M. Magini, S. Martelli and F. Padella: Il Nuovo Cimento, **13** (1991).
2. M. Abdellaoui and E. Gaffet: Journal of Alloys and Compounds, 1119 (1994)
3. D. I. Hoyer: Int. Conf. on Recent Advances in Mineral Sciences and Technology, Mintek,(1984).
4. P. A. Cundall and O. D. L. Strack: Geotechnique **29** (1979).
5. B. K. Mishra and R. K. Rajamani: KONA Powder and Particle, **8** (1990).
6. B. K. Mishra and R. K. Rajamani: Appl. Math. Modelling, **16**, (1992).
7. J. L. Meriam and L. G. Kraig: Engineering Mechanics, John Wiley & Sons, New York, (1987).
8. M.P. Dallimore and McCormick: Materials Transactions, JIM, Hawaii meeting, in press.
9. H. Huang: The Dynamics of Mechanical Milling. PhD Thesis, University of Western Australia, (1995).
10. A. Iasonna and M. Magini: Acta mater., Vol 44, No. 3, (1996).
11. P. G. McCormick, H. Huang, M. P. Dallimore, J. Ding and J. Pan: Proceedings of 2nd International Conference of Structural Applications of Mechanical Alloying, Vancouver, Canada, September 20-22, 1993.